JACS
JOURNAL OF THE AMERICAN CHEMICAL SOCIETY

Subscriber access provided by ISTANBUL TEKNIK UNIV

Article

To Dope or Not To Dope: The Effect of Sonicating Single-Wall Carbon Nanotubes in Common Laboratory Solvents on Their Electronic Structure

Kevin R. Moonoosawmy, and Peter Kruse

J. Am. Chem. Soc., **2008**, 130 (40), 13417-13424 • DOI: 10.1021/ja8036788 • Publication Date (Web): 13 September 2008

Downloaded from http://pubs.acs.org on February 8, 2009

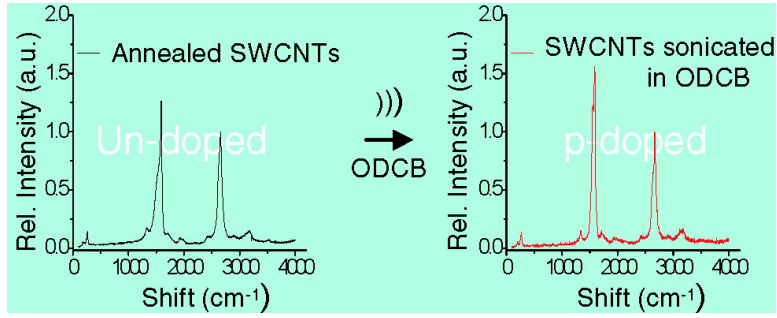

More About This Article

Additional resources and features associated with this article are available within the HTML version:

- Supporting Information
- Links to the 1 articles that cite this article, as of the time of this article download
- Access to high resolution figures
- Links to articles and content related to this article
- Copyright permission to reproduce figures and/or text from this article

View the Full Text HTML

ACS Publications
High quality. High impact.

Journal of the American Chemical Society is published by the American Chemical Society. 1155 Sixteenth Street N.W., Washington, DC 20036

J|A|C|S
ARTICLES

Published on Web 09/13/2008

To Dope or Not To Dope: The Effect of Sonicating Single-Wall Carbon Nanotubes in Common Laboratory Solvents on Their Electronic Structure

Kevin R. Moonoosawmy and Peter Kruse*

Department of Chemistry, McMaster University, 1280 Main Street West, Hamilton, Ontario L8S 4M1, Canada

Received May 16, 2008; E-mail: pkruse@mcmaster.ca

Abstract: Single-wall carbon nanotubes (SWCNTs) are commonly dispersed via sonication in a solvent prior to functionalization. We show that solvents such as dichloromethane, chloroform, 1,2-dichloroethane, and *o*-dichlorobenzene lead to an upward shift in the Raman response of the SWCNTs. We have used *o*-dichlorobenzene as a model molecule to explain this effect, and an upward shift of 9 cm^{-1} is observed in the D* band. This blue shift is associated with p-type doping and is triggered only when the nanotubes are sonicated in the solvent. Sonication decomposes the chlorinated solvents, and new species (Cl_2 and HCl(g)) are formed. The catalytic Fe nanoparticles inherently present in the nanotubes are etched by chlorine and hydrogen chloride to form iron chlorides during sonication in the solvent. The dopant was identified by X-ray photoelectron spectroscopy. With such knowledge of doping, the choice of solvent becomes crucial for any chemical reaction and can be intentionally tuned to produce SWCNTs films for electronics applications.

1. Introduction

Single-wall carbon nanotubes (SWCNTs) are quasi-one-dimensional structures that have desirable electronic properties, very good mechanical strength, and high thermal stability.[1] Therefore, they have numerous potential applications ranging from composite materials[2] to chemical sensors.[3,4] Current bulk syntheses of SWCNTs, such as the HiPco process, generate ropes and bundles.[5] Therefore, bulk processability requires sonication to disperse SWCNTs in a solvent. Such a wet-chemical process is an essential step for the purification,[6−8] separation (semiconducting from metallic SWCNTs),[9−14] functionalization (modification of their band gap),[15] and doping[16] of the SWCNTs.

SWCNTs are sensitive to their chemical environment. Amines,[17] ammonia, nitrogen dioxide,[18] and oxygen[19,20] are all known to alter their electronic properties. Electron donors such as ammonia and alkylamines,[17,21] adsorbed on SWCNTs, lead to n-doping. Intercalation of alkali metals into SWCNTs also leads to n-doping.[22−28] This was observed to produce a softening

(1) Dresselhaus, M. S.; Dresselhaus, G.; Eklund, P. C. *Science of Fullerenes and Carbon Nanotubes*; Academic: San Diego, CA, 1996.
(2) Schaefer, D. W.; Justice, R. S. *Macromolecules* **2007**, *40*, 8501–8517.
(3) Avouris, P. *Acc. Chem. Res.* **2002**, *35*, 1026–1034.
(4) Avouris, P.; Appenzeller, J. *The Industrial Physicist* **2004**, *10*, 18–21.
(5) Nikiloev, P.; Bronikowski, M. J.; Bradley, R. K.; Rohmund, F.; Colbert, D. T.; Smith, K. A.; Smalley, R. E. *Chem. Phys. Lett.* **1999**, *313*, 91–97.
(6) Yu, A.; Bekyarova, E.; Itkis, M. E.; Fakhrutdinov, D.; Webster, R.; Haddon, R. C. *J. Am. Chem. Soc.* **2006**, *128*, 9902–9908.
(7) Liu, J.; Rinzler, A. G.; Dai, H.; Hafner, J. H.; Bradley, R. J.; Boul, P. J.; Lu, A.; Iverson, T.; Shelimov, K.; Huffman, C. B.; Rodriguez-Macias, F.; Shon, Y. S.; Lee, T. R.; Colbert, D. T.; Smalley, R. E. *Science* **1998**, *280*, 1253–1256.
(8) Chiang, I. W.; Brinson, B. E.; Huang, A. Y.; Willis, P. A.; Bronikowski, M. J.; Margrave, J. L.; Smalley, R. E.; Hauge, R. H. *J. Phys. Chem. B* **2001**, *105*, 8297–8301.
(9) Chen, Z.; Du, X.; Du, M. H.; Rancken, C. D.; Cheng, H. P.; Rinzler, A. G. *Nano Lett.* **2003**, *3*, 1245–1249.
(10) Samsonidze, G. G.; Chou, S. G.; Santos, A. P.; Brar, V. W.; Dresselhaus, G.; Dresselhaus, M. S.; Selbst, A.; Swan, A. K.; Unlu, M. S.; Goldberg, B. B.; Chattopadhyay, D.; Kim, S. N.; Papadimitrakopoulos, F. *Appl. Phys. Lett.* **2004**, *85*, 1006–1008.
(11) Brar, V. W.; Samsonidze, G. e. G.; Santos, A. P.; Chou, S. G.; Chattopadhyay, D.; Kim, S. N.; Papadimitrakopoulos, F.; Zheng, M.; Jagota, A.; Onoa, G. B.; Swan, A. K.; Ünlü, M. S.; Goldberg, B. B.; Dresselhaus, G.; Dresselhaus, M. S. *J. Nanosci. Nanotechnol.* **2005**, *5*, 209–228.
(12) Banerjee, S.; Hemraj-Benny, T.; Wong, S. S. *J. Nanosci. Nanotechnol.* **2005**, *5*, 841–855.
(13) Arnold, M. S.; Stupp, S. I.; Hersam, M. C. *Nano Lett.* **2005**, *5*, 713–718.
(14) Krupke, R.; Linden, S.; Rapp, M.; Hennrich, F. *Adv. Mater.* **2006**, *18*, 1468–1470.
(15) Strano, M. S.; Dyke, C. A.; Usrey, M. L.; Barone, P. W.; Allen, M. J.; Shan, H.; Kittrell, C.; Hauge, R. H.; Tour, J. M.; Smalley, R. E. *Science* **2003**, *301*, 1519–1522.
(16) Dettlaff-Weglikowska, U.; Skakalova, V.; Graupner, R.; Jhang, S. H.; Kim, B. H.; Lee, H. J.; Ley, L.; Park, Y. W.; Berber, S.; Tomanek, D.; Roth, S. *J. Am. Chem. Soc.* **2005**, *127*, 5125–5131.
(17) Kong, J.; Dai, H. *J. Phys. Chem. B* **2001**, *105*, 2890–2893.
(18) Kong, J.; Franklin, N. R.; Zhou, C. W.; Chapline, M. G.; Peng, S.; Cho, K. J.; Dai, H. *Science* **2000**, *287*, 622–625.
(19) Collins, P. G.; Bradley, K.; Ishigami, M.; Zettl, A. *Science* **2000**, *287*, 1801–1804.
(20) Chen, R. J.; Franklin, N. R.; Kong, J.; Cao, J.; Tombler, T. W.; Zhang, Y.; Dai, H. *Appl. Phys. Lett.* **2001**, *79*, 2258–2260.
(21) Shim, M.; Javey, A.; Shi Kam, N. W.; Dai, H. *J. Am. Chem. Soc.* **2001**, *123*, 11512–11513.
(22) Lee, R. S.; Kim, H. J. *Nature* **1997**, *388*, 255.
(23) Lee, R. S.; Kim, H. J.; Fischer, J. E.; Lefebvre, J.; Radosavljevic, M.; Johnson, A. T. *Phys. Rev. B* **2000**, *61*, 4526–4529.
(24) Claye, A. S.; Fischer, J. E.; Huffman, C. B.; Rinzler, A. G.; Smalley, R. E. *J. Electrochem. Soc.* **2000**, *147*, 2845–2852.
(25) Rao, A. M.; Eklund, P. C.; Bandow, S.; Thess, A.; Smalley, R. E. *Nature* **1997**, *388*, 257–259.

 © 2008 American Chemical Society

of the tangential mode (G mode ~1590 cm^{-1})[25,26] of the Raman spectra. Electron-withdrawing molecules, such as oxygen,[19] thionyl chloride,[16,29] $FeCl_3$,[30] Brønsted acids[31] and solid organic acids,[32] all lead to p-doping of the SWCNTs. Intercalation of halogens molecules such as I_2 and Br_2 has also been shown to cause p-type doping.[26,27,33] Encapsulation of electrophilic organic molecules, such as tetracyanoquinodimethane (TCNQ) and tetrafluorotetracyanoquinodimethane ($TCNQF_4$), p-dopes the SWCNTs; conversely, nucleophilic molecules, such as tetrathiafulvalene (TTF) and tetrakis(dimethylamino)ethylene (TDAE), n-dope the SWCNTs.[34−37] In analogy to the intercalation of various compounds in graphite,[38,39] the electrical conductivity of SWCNTs can be modified by either electron donors or electron acceptors.

A wet chemical process is routinely used to disperse SWCNTs. *o*-Dichlorobenzene (ODCB) has been regarded as the most suitable solvent for dispersion when compared to other common laboratory solvents.[40] For example, SWCNTs are sonicated in ODCB[41] prior to functionalization in the Bingel reaction[42,43] and the diazonium reaction.[41] 1,2-Dichloroethane (DCE) has more recently also found use as a dispersant medium.[44,45] However, little attention has been given to understanding the impact of sonication on solvents (such as halogenated ones) used for dispersion and how this affects the electronic structure of the SWCNTs.

We have studied the effect of chlorinated organic molecules on the electronic structure of SWCNTs upon sonication. Organic halides are known to decompose during sonication to liberate halogens and polymerize.[46,47] We have used ODCB as a model molecule to elucidate the origin of the effect and further confirm which compound caused a change in the electronic structure. The doping effect was also investigated by contrasting several laboratory solvents commonly used in conjunction with SWCNTs. The chemical modification that ensued on the SWCNT network has been characterized by Raman spectroscopy and X-ray photoelectron spectroscopy (XPS). Its origins have been examined by gas chromatography/mass spectrometry (GC-MS), titrimetric methods, matrix-assisted laser desorption/ionization time-of-flight (MALDI-TOF), thermogravimetric analysis (TGA), and inductively coupled plasma mass spectrometry (ICP-MS).

2. Sample Preparation and Experimental Methods

The single-wall carbon nanotubes (SWCNTs) were purchased from Carbon Nanotechnologies Inc. (Houston, TX). The as-received SWCNTs were annealed at 800 °C for 1 h under vacuum following a very slow ramp at a rate of 1 °C/min. The annealed SWCNTs were preserved in a vial that was stored under Ar. This procedure removes any contaminants from the SWCNTs. Two batches of HiPco SWCNTs were used (batch no. PO257, 14 wt % total residual content; batch no. PO343, 5 wt % total residual content). Most of the chemicals were purchased from Sigma-Aldrich, except for DCM, MeOH (Fisher), and THF (Caledon). The gases were purchased from Praxair Inc. (anhyd. 99.0% HCl), Vitalaire (99.99% UHP-grade Ar), and Air Liquide Canada (2 mol % Cl_2/Ar gas mixture). A summary of the grade and purity of each chemical is provided in the Supporting Information. The chemicals were used as received unless otherwise stated. A polytetrafluoroethylene (PTFE) filter membrane (0.2 μm) from Pall Life Science was used throughout this study.

2.1. Dispersion of the SWCNTs. Sonication was carried out in a 42 kHz bath sonicator (Branson 1510, 70 W). All of the sonication experiments were performed under ambient conditions for 1 h. The temperature of the water bath was routinely observed to change after an hour, from room temperature to within a range of 32−38 °C. Argon gas, maintained by an inflated balloon, created an inert atmosphere inside the sonication vessel. Flame-dried round-bottom flasks (RBFs) were used for all sonication steps. The shape of the vessel has previously been suggested to have an effect on the intensity of sonication.[46] The vessel was consistently positioned in the middle of the bath in the region of highest visible agitation. Stirring was carried out in flamed-dried RBFs under an Ar atmosphere for 1 h using a 0.5 in. PTFE-coated stirring magnet. Some neat solvent samples were presonicated for 1 h under Ar in the absence of SWCNTs. Cl_2/Ar (2 mol %) gas mixture was slowly bubbled into 15 mL of ODCB for 1 h. Alternatively, hydrogen chloride (anhyd. 99.0%) was also bubbled into a separate portion of 15 mL of ODCB for 10 min. Argon gas was used to purge-off the gases (Cl_2 and HCl(g) respectively) from a 7.5 mL portion of the previously prepared solvents for 5 h to ensure maximum degassing. A very small amount of SWCNTs (5 mg) was added to the solvent (7.5 mL) and agitated via sonication or stirring under Ar for 1 h. The dispersion was then filtered over 0.2 μm PTFE membrane. A film was formed only when the SWCNTs were sonicated. The stirred samples produced a granular residue once they were filtered over the PTFE membrane.

2.2. Instrumentation. Raman spectra were acquired using a Renishaw 2000 microscope, with a spectral resolution of 2 cm^{-1}, using a backscattering configuration with a 50× objective excited with an Ar^+ ion laser at 514 nm (2.41 eV). Data were collected on numerous spots (10 spots) on the sample and recorded with a fully

(26) Rao, A. M.; Bandow, S.; Richter, E.; Eklund, P. C. *Thin Solid Films* **1998**, *331*, 141–147.
(27) Kazaoui, S.; Minami, N.; Jacquemin, R.; Kataura, H.; Achiba, Y. *Phys. Rev. B* **1999**, *60*, 13339–13342.
(28) Kim, Y. A.; Kojima, M.; Muramatsu, H.; Umemoto, S.; Watanabe, T.; Yoshida, K.; Sato, K.; Ikeda, T.; Hayashi, T.; Endo, M.; Terrones, M.; Dresselhaus, M. S. *Small* **2006**, *2*, 667–676.
(29) Skakalova, V.; Kaiser, A. B.; Dettlaff-Weglikowska, U.; Hrncarikova, K.; Roth, S. *J. Phys. Chem. B* **2005**, *109*, 7174–7181.
(30) Liu, X.; Pichler, T.; Knupfer, M.; Fink, J.; Kataura, H. *Phys. Rev. B* **2004**, *70*, 205405.
(31) Graupner, R.; Abraham, J.; Vencelova, A.; Seyller, T.; Hennrich, F.; Kappes, M. M.; Hirsch, A.; Ley, L. *Phys. Chem. Chem. Phys.* **2003**, *5*, 5472–5476.
(32) Klinke, C.; Afzali, A.; Avouris, P. *Chem. Phys. Lett.* **2006**, *430*, 75–79.
(33) Grigorian, L.; Williams, K. A.; Fang, S.; Sumanasekera, G. U.; Loper, A. L.; Dickey, E. C.; Pennycook, S. J.; Eklund, P. C. *Phys. Rev. Lett.* **1998**, *80*, 5560–5563.
(34) Lu, J.; Nagase, S.; Yu, D.; Ye, H.; Han, R.; Gao, Z.; Zhang, S.; Peng, L. *Phys. Rev. Lett.* **2004**, *93*, 116804.
(35) Takenobu, T.; Takano, T.; Shiraishi, M.; Murakami, Y.; Ata, M.; Kataura, H.; Achiba, Y.; Iwasa, Y. *Nat. Mater.* **2003**, *2*, 683–688.
(36) Kazaoui, S.; Minami, N.; Kataura, H.; Achiba, Y. *Synth. Met.* **2001**, *121*, 1201–1202.
(37) Kazaoui, S.; Guo, Y.; Zhu, W.; Kim, Y.; Minami, N. *Synth. Met.* **2003**, *135−136*, 753–754.
(38) Conard, J. Electronic structure of various forms of solid state carbons. Graphite intercalation compounds. In *New Trends in Intercalation Compounds for Energy Storage*; Julien, C., Pereira-Ramos, J. P., Momchilov, A., Eds.; NATO Science Series, II: Mathematics, Physics and Chemistry; Kluwer Academic Publishers: Amsterdam, 2002; pp 39−62.
(39) Dresselhaus, M. S.; Dresselhaus, G. *Adv. Phys.* **2002**, *51*, 1–186.
(40) Bahr, J. L.; Mickelson, E. T.; Bronikowski, M. J.; Smalley, R. E.; Tour, J. M. *Chem. Commun.* **2001**, 193–194.
(41) Bahr, J. L.; Tour, J. M. *Chem. Mater.* **2001**, *13*, 3823–3824.
(42) Worsley, K. A.; Moonoosawmy, K. R.; Kruse, P. *Nano Lett.* **2004**, *4*, 1541–1546.
(43) Coleman, K. S.; Bailey, S. R.; Fogden, S.; Green, M. L. H. *J. Am. Chem. Soc.* **2003**, *125*, 8722–8723.
(44) Kim, K. K.; Bae, D. J.; Yang, C.-M.; An, K. H.; Lee, J. Y.; Lee, Y. H. *J. Nanosci. Nanotechnol.* **2005**, *5*, 1055–1059.
(45) Li, X.; Zhang, L.; Wang, X.; Shimoyama, I.; Sun, X.; Seo, W.-S.; Dai, H. *J. Am. Chem. Soc.* **2007**, *129*, 4890–4891.
(46) Niyogi, S.; Hamon, M. A.; Perea, D. E.; Kang, C. B.; Zhao, B.; Pal, S. K.; Wyant, A. E.; Itkis, M. E.; Haddon, R. C. *J. Phys. Chem. B* **2003**, *107*, 8799–8804.
(47) Srivastava, S. C. *Nature* **1958**, *182*, 47.

focused 1% laser power having a spot size of ~1.2 μm; the latter has a power density of ~10 $\mu W/\mu m^2$ at the sample. In order to visually aid comparison within and among the samples, all Raman spectra were scaled with respect to the intensity of the second-order peak at ~2660 cm^{-1}.

The XPS analyses were performed using a Kratos Axis Ultra spectrometer with a monochromatic Al Kα source (15 mA, 1486.6 eV). The SWCNTs samples (powder and thin films) were pressed onto indium foil for analysis. XPS probes the surface of the sample to a depth of 7−10 nm and has detection limits ranging from 0.1 to 0.5 atom %, depending on the element. The instrument work function was calibrated to give a binding energy (BE) of 83.96 eV for the Au 4f7/2 line for metallic gold, and the spectrometer dispersion was adjusted to give a BE of 932.62 eV for the Cu 2p3/2 line of metallic copper. The Kratos charge neutralizer system was not employed. High-resolution (0.1 eV) spectra were obtained using a 20 eV pass energy and an analysis area of ~300 × 700 μm.

GC-MS was used to examine changes, such as dimerization in the solvent after it was freshly sonicated, using a Varian 1200 GC-EI/CI triple-quadrupole mass spectrometer. A Micromass MALDI MicroMX mass spectrometer was used to analyze the supernatant solvent that was allowed to stand for a week.

Chlorine and hydrogen chloride were detected titrimetrically. The sonicated ODCB was washed with 3 × 5 mL of boiled Millipore water (18 MΩ, pH = 7) to extract the acid into the aqueous phase. Bromothymol blue was used as an indicator. After extraction and addition of the indicator, the yellow aqueous phase was titrated with NaOH (4×10^{-4} M) until neutrality (green coloration) was achieved. The presence of chlorine was detected using the same protocol, but potassium iodide (3 × 5 mL; 0.05 M) solution was used instead of water and starch was used as an indicator. Potassium iodide is oxidized by chlorine to produce iodine, which turns blue upon addition of starch as an indicator.

Iron content was determined by heating 1 mg of SWCNTs to 1100 °C in air using a Netzsch STA 409 Luxx thermal analyzer. The residual material was digested using hot chloric acid (26 wt %) according to a literature protocol.[48,49] The resulting solution was diluted to 25 mL with 1 wt % HNO_3(aq), and the Fe content was determined using an Elan 6000 ICP mass spectrometer from PerkinElmer.

3. Results and Discussion

3.1. Effect of Ambient Conditions on Annealed SWCNTs. Raman spectra were collected over a range from 100 to 4000 cm^{-1} to include the Raman feature at ~2660 cm^{-1}. The intensity of this peak will be used to scale the spectrum and facilitate the visual comparison between spectra. Single crystals of carbon nanotubes do not exist, and their full phonon dispersion cannot be found experimentally.[50] Due to the nature of carbon nanotube networks, an internal standardization protocol is still lacking for spectral calibration. The choice of the feature at ~2660 cm^{-1} is discussed later.

Since SWCNTs are sensitive to their chemical environment, they were decontaminated by annealing and then stored under Ar. To validate the effectiveness of the annealing step, three samples (A, B, C) from the same batch were compared. Samples A and B were annealed, whereas sample C was left unannealed. Samples A and C were pressed onto a PTFE membrane for data collection in air, whereas sample B was placed inside a capillary tube.

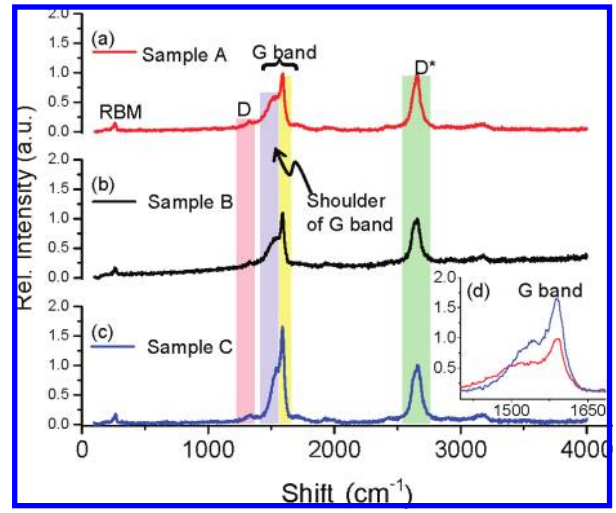

Figure 1. Raman spectra of annealed SWCNTs: (a) sample A (red) pressed onto a PTFE membrane, (b) sample B (black) in a sealed capillary tube, and (c) as-is unannealed SWCNTs, sample C (blue), also pressed onto a PTFE membrane. The inset (d) corresponds to the G band of samples A and C, respectively.

Four distinct features are observed from the SWCNTs spectrum, as can be seen in Figure 1a: the features appearing between 100 and 300 cm^{-1} are labeled the radial breathing mode (RBM); the D peak is observed at ~1350 cm^{-1}; the G band is observed in the region of 1400−1700 cm^{-1}; and the D* mode is observed in the range of 2500−2800 cm^{-1}.[50] The RBM is a fingerprint signal indicating the presence of SWCNTs with different diameters and chiralities. In this work we have focused our attention on the G-band and the D* mode. The asymmetric shoulder at 1540 cm^{-1} on the G band is due to electron−phonon coupling in bundles of SWCNTs, which is a characteristic of metallic nanotubes.[50,51] The nature of the D* mode is discussed in section 3.2.

Sample B, collected inside a capillary tube, shows strong fluorescence because of the glass when compared to the spectrum of sample A (Figure 1b). Despite the fluorescence in sample B, both annealed samples A and B correlate well with each other. Figure 1c is the spectrum of the unannealed sample C and was collected on a filter membrane. The shoulder of the G band at about 1540 cm^{-1} is less broad than for the annealed samples A and B. By comparing the G band feature of samples A (annealed) to C (unannealed), a difference in the spectra is visible (inset Figure 1d). The G band of the unannealed sample C has a higher intensity, and the shoulder is narrower. Contaminations from the laboratory environment can affect the integrity of the SWCNTs sample and can be removed by annealing. Sample A was chosen as our reference annealed SWCNTs for the following discussion.

3.2. Sonication Leads to Doping. Two samples of annealed SWCNTs were treated with ODCB using two different agitation methods: sonication and stirring, respectively. Two other samples were prepared similarly, but toluene was used as a non-chlorinated aromatic solvent for comparison. The Raman spectrum for each sample was collected. The sonicated samples, once filtered over the PTFE membrane, afford a homogeneous film, whereas the stirred samples produce granules.

All spectra were collected with the sample on a PTFE membrane and are scaled with respect to the D* peak intensity

(48) Mackeyev, Y.; Bachilo, S.; Hartman, K. B.; Wilson, L. J. *Carbon* **2007**, *45*, 1013–1017.
(49) Lamb, A. B.; Bray, W. C.; Geldard, W. I. *J. Am. Chem. Soc.* **1920**, *42*, 1636–1648.
(50) Reich, S.; Thomsen, C.; Maultzsch, J. *Carbon nanotubes: Basic concepts and physical properties*; Wiley-VCH Verlag: Berlin, 2004.
(51) Caudal, N.; Saitta, A. N.; Lazzeri, M.; Mauri, F. *Phys. Rev. B* **2007**, *75*, 115423.

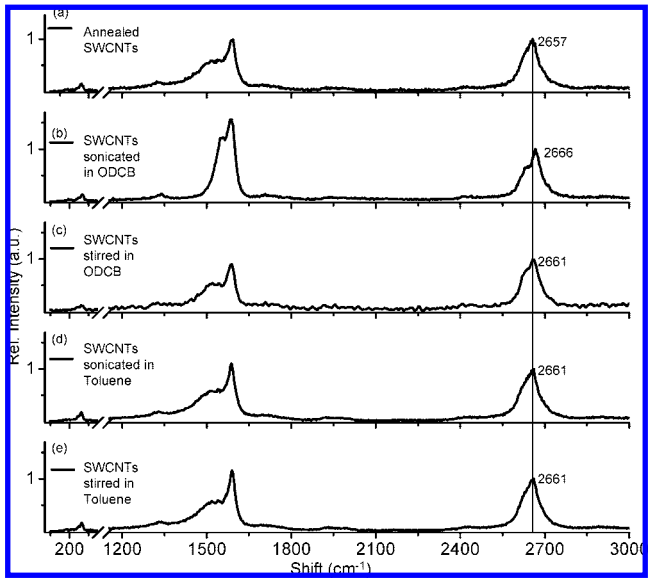

Figure 2. Raman spectra of (a) annealed pristine SWCNTs, (b) SWCNTs sonicated in ODCB, (c) SWCNTs stirred in ODCB, (d) SWCNTs stirred in toluene, and (e) SWCNTs sonicated in toluene.

at about 2660 cm^{-1}. It is reported to be a second-order peak arising from the scattering of large q vectors ($q > 0$) via a double-resonance process.[50] The process involves either inelastic scattering of two phonons with wave vectors of opposite sign, $\pm q$ (second-order Raman scattering), or elastic scattering by defects.[52] The D* is assigned to be an overtone of the D peak, as they are both dispersive peaks that shift by 90 ± 3 and 38 ± 2 cm^{-1}/eV, respectively, with laser energy.[53] The intensity of the second-order overtone (D*), in principle, does not depend on defect concentration, but it is affected equally by those effects that influence the first-order or higher order scatterings.[50,54] Previously, Corio et al.[55] have reported that a shift in the D* peak is indicative of electron charge transfer from the carbon atoms of SWCNTs to the adsorbates. This would provide a means to gauge the effect of dopants on the SWCNTs network.

The SWCNTs sample sonicated in ODCB affords a spectrum that is significantly different from the other spectra, as seen in Figure 2b. There are three features observed in that spectrum that we relate to doping behavior when compared to the Raman spectrum of an annealed reference SWCNTs sample: (1) The shoulder (asymmetry) of the G band at about 1540 cm^{-1} is lost (Figure 2b). (2) The peak at about 1600 cm^{-1} in the G band increases in relative intensity (Figure 2b). (3) The D* peak shifts upward by 9 cm^{-1}(Figure 2 b).

The other spectra, as seen in Figure 2c,e, do not show any loss in the shoulder of the G band, and the relative intensity of the G band, with respect to the D* peak, does not increase. A slight shift of 4 cm^{-1} is observed in the D* peak, as seen in Figure 2d,e, and is attributed to the aggregation[56,57] of the SWCNTs network in the thin film formed after sonication. Thence, toluene did not significantly affect the Raman spectrum of the SWCNTs whether sonicated or stirred, whereas ODCB changed the Raman spectrum of the SWCNTs only when sonicated.

The interactions between SWCNT bundles are reduced due to charge transfer, and thus the suppression of the shoulder in Figure 2b is attributed to changes in the electronic properties leading to different electron−phonon coupling. The electronic structure of the SWCNTs has been modified, but no covalent bond is formed, as the intensity of the D peak at about 1350 cm^{-1} does not increase. Therefore, the blue shift in the D* peak is assigned to noncovalent interactions between the adsorbates and the SWCNTs, leading to electron transfer from the carbon atoms of the SWCNTs to the adsorbates. Thus, ODCB leads to p-doping of the SWCNTs.

Similarly, the Raman spectra of SWCNTs treated with thionyl chloride[16] and sulfuric acid[55] show distinctive upward shifts that have been attributed to p-doping. Corio et al.[55] have used the shift in the D* mode as a gauge of charge transfer when SWCNTs are electrochemically treated with H_2SO_4. Upward shifts in Raman features such as in the G band have also been observed when the SWCNTs are heavily p-doped by intercalating I_2 and Br_2,[26] but unfortunately, no values were recorded for the D* mode. Our data can explain shifts in the Raman features that were unaccounted for by Niyogi et al.[46]

The main impurity in anhydrous ODCB is *p*-dichlorobenzene,[58] with trace amounts of water (0.005%) and evaporation residues (0.0003%) (see Supporting Information for certificate of analysis). By stirring the ODCB with SWCNTs, we found that neither ODCB nor these impurities lead to doping of the SWCNTs by their shear presence only. ODCB has also been purified, according to literature,[59] and the resulting solvent also showed doping only when sonicated (Supporting Information, S1).

3.3. Understanding the Pathway by Which Sonication Leads to Doping. Since sonication is the only pathway by which doping is achieved, identification of the species formed during sonication is required. Sonication is known to promote the decomposition of organic solvents.[46] Organic halides are known to decompose during sonication to liberate halogens and polymerize.[47] GC-MS of the freshly sonicated neat ODCB showed several new peaks when compared to that of the neat, unsonicated ODCB (Supporting Information, S2). The species are mostly mono-, bis-, and trichlorinated biphenyls. The reflectron MALDI-TOF spectrum of the supernatant liquid from the sonicated neat ODCB (left standing for a week) is shown in Figure 3. The peaks with highest intensity are separated by a constant m/z of 74.02, suggesting an aromatic ring repeat unit with four bonds. ODCB undergoes sonochemical polymerization when sonicated via a radical pathway following the cleavage of the C−Cl bond. The polymerization occurs over time; a MALDI-TOF spectrum of a freshly sonicated sample does not show any conclusive signs of polymeric material. The $Cl^{\bullet}$ radicals abstract a hydrogen, producing hydrogen chloride, and a propagation reaction leads to the formation of the polymer; chlorine gas can be formed by the combination of two $Cl^{\bullet}$.

The presence of hydrogen chloride and chlorine was separately detected titrimetrically. After the extraction of hydrogen

(52) Reich, S.; Thomsen, C. *Philos. Trans. R. Soc.* **2004**, *362*, 2271–2288.
(53) Thomsen, C. *Phys. Rev. B* **2000**, *61*, 4542LP–4544LP.
(54) Curran, S. A.; Talla, J. A.; Zhang, D.; Carroll, D. L. *J. Mater. Res.* **2005**, *20*, 3368–3373.
(55) Corio, P.; Santos, P. S.; Brar, V. W.; Samsonidze, G. G.; Chou, S. G.; Dresselhaus, M. S. *Chem. Phys. Lett.* **2003**, *370*, 675–682.
(56) Strano, M. S.; Ursey, M. L.; Barone, P. W.; Heller, D. A.; Baik, S. The selective chemistry of single walled carbon nanotubes. In *Applied Physics of Carbon Nanotubes, Fundamentals of Theory, Optics and Transport Devices*; Rotkin, S. V., Subramoney, S., Eds.; Springer: Berlin, 2005; pp 151−180.
(57) Heller, D. A.; Barone, P. W.; Swanson, J. P.; Mayrhofer, R. M.; Strano, M. S. *J. Phys. Chem. B* **2004**, *108*, 6905–6909.
(58) Weissberger, A.; ProskauerE. *Organic solvents: physical constants and methods of purification*; Clarendon Press: Oxford, 1935; p 158.
(59) Suslick, K. S.; Fox, M. M.; Reinert, T. R. *J. Am. Chem. Soc.* **1984**, *106*, 4522–4525.

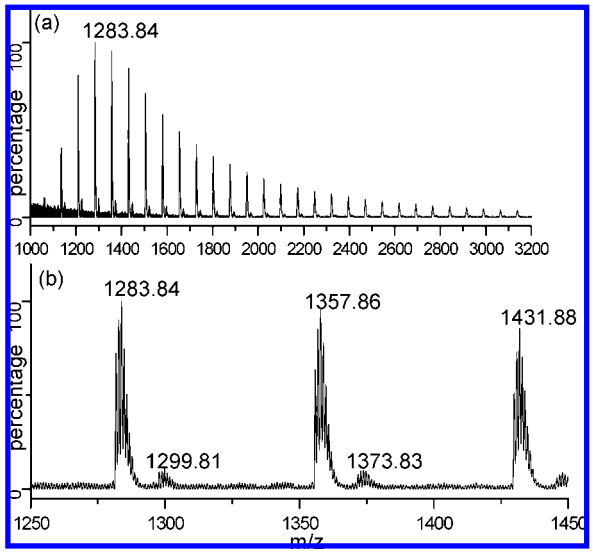

Figure 3. (a) Reflectron MALDI-TOF spectrum of sonicated ODCB and (b) high-resolution scan of the peak around 1283.84. The highest intensity peaks are separated by a constant *m*/*z* of 74.02.

chloride with Millipore water, the aqueous phase turned yellow upon addition of the indicator (bromothymol blue). The acid concentration in the aqueous phase was found to be 3×10^{-5} M when titrated with NaOH (4×10^{-4} M). We conclude that the presence of acid was proven qualitatively since the partition coefficient of the acid from the organic phase into the aqueous phase was not considered. The presence of chlorine is qualitatively detected by using potassium iodide solution (0.05 M KI). Quantification was not pursued due to the heterogeneous nature of the two solvents and an undefined partition coefficient. The aqueous phase turned blue upon addition of starch as indicator due to the presence of iodine. Chlorine oxidized the iodide ions to iodine. Hence, the presence of the iodine was confirmed, implying the presence of chlorine. There was no color change with neat ODCB. Sonication leads to the formation of new species such as hydrogen chloride and chlorine, and these trigger the doping effect.

Triggering the radical pathway is just the first step; its interruption is the next corollary step toward understanding it. Alcohols are often added to organic solvents to stabilize them and, at certain concentrations, can quench the decomposition, which is believed to go through a radical pathway.[46,47] Methanol, a radical quencher, is used to investigate whether it inhibits the doping effect during sonication. SWCNTs sonicated in methanol do not show any signs of doping (Supporting Information, S3). The doping effect is suppressed when 1 wt % methanol in ODCB is used to sonicate the SWCNTs. The shoulder of the G band is still present, and the D* peak does not shift (Supporting Information, S3). The C−Cl (394.9 kJ/mol)[60] bond is cleaved during sonication,[47] and $Cl^{\bullet}$ radicals are formed. The quenching experiment shows that the doping effect can be suppressed, as the radicals formed during sonication are scavenged by methanol. In contrast, adding 5 wt % toluene in ODCB did not suppress the doping effect, as it does not quench the radical.

Since sonication is the only agitation method yielding this doping behavior, several questions arise. Radicals are formed during sonication, thereby initiating sonochemical polymerization and formation of new species such as chlorine and hydrogen chloride.[61] Which of these species lead to doping? Is doping a direct consequence of their shear presence, or do they react further with the catalytic material inherently present? The following experiments answer those questions and help us elucidate which species leads to doping.

3.4. Hydrogen Chloride and Chlorine Lead to Doping. ODCB is presonicated to generate the polymer along with the other species. It is then stirred with the SWCNTs for 1 h under Ar. Stirring is preferred in this case, as resonication will further decompose the monomers still present in the mixture. Another sample of ODCB is presonicated and then purged with Ar to degas it and leave only the polymeric material in the mixture, prior to stirring with SWCNTs.

The Raman spectra of these two samples are shown in Figure 4a,b, respectively. The presonicated material dopes the SWCNTs when the mixture is stirred. However, when the presonicated material is purged with Ar prior to stirring with the SWCNTs, the Raman spectrum shows no sign of doping, as shown in Figure 4b. This indicates that the species leading to doping can be purged off. We thus exclude the polymeric material as being the dopant.

Chlorine and hydrogen chloride gases are formed during sonication[47,61] of ODCB and lead to doping of the SWCNTs. To replicate this process, a 2 mol % Cl_2/Ar gas mixture was bubbled into ODCB. The colorless solution turned yellowish during the bubbling procedure. Sonication of neat ODCB also produced a similar color change within minutes. The chlorinated solution was stirred with the SWCNTs, and the resulting Raman spectrum confirmed prominent doping features, as shown in Figure 4c. The dopant can be removed by purging the chlorinated solution with Ar. The solution changed color from a pale yellow tint to colorless within 10 min but subsequently turned to a permanent yellow color after 1 h. This degassed solvent did not dope the SWCNTs when the mixture was stirred, as can be seen in Figure 4d.

Anhydrous hydrogen chloride (99.0%) was also bubbled into ODCB. The solution did not change color, and the solvent mixture doped the SWCNTs upon stirring, as shown in Figure 4e. After the solvent was degassed with Ar and stirred with SWCNTs, the Raman response showed no signs of doping, as seen in Figure 4f. Degassing the solvent with Ar (Figure 4g−i) has the effect of decreasing the relative intensity of the G band after the gas (Cl_2/HCl) was purged off. The D* peak shows an upward shift (p-doping) in the presence of a species leading to doping; however, no such shift was observed with the degassed solvent (Figure 4j−l).

3.5. Effect of Other Common Solvents on the Raman Response of SWCNTs. ODCB leads to doping of the SWCNTs when sonicated due to the formation of gases such as chlorine and hydrogen chloride. The solvent also forms polymeric material after sonication. We expanded our study to other organic solvents commonly used during the wet processing of SWCNTs, such as dichloromethane (DCM), chloroform ($CHCl_3$), carbon tetrachloride (CCl_4), 1,2-dichloroethane (1,2-DCE), chlorobenzene (Cl-Ph), 1-chlorobutane (1-Cl-But), tetrahydrofuran (THF), methanol (MeOH), ethanol (EtOH), and dimethylformamide (DMF).

(60) Luo, Y. R. Bond Dissociation Energies. In *CRC Handbook of Chemistry and Physics*, 87th ed.; Lide, D. R., Ed.; Taylor and Francis: Boca Raton, FL, 2007; Internet Version, 9-56−9-80.

(61) Mhuircheartaigh, É. M. N.; Blau, W. J.; Prato, M.; Giordani, S. *Carbon* **2007**, *45*, 2665–2671.

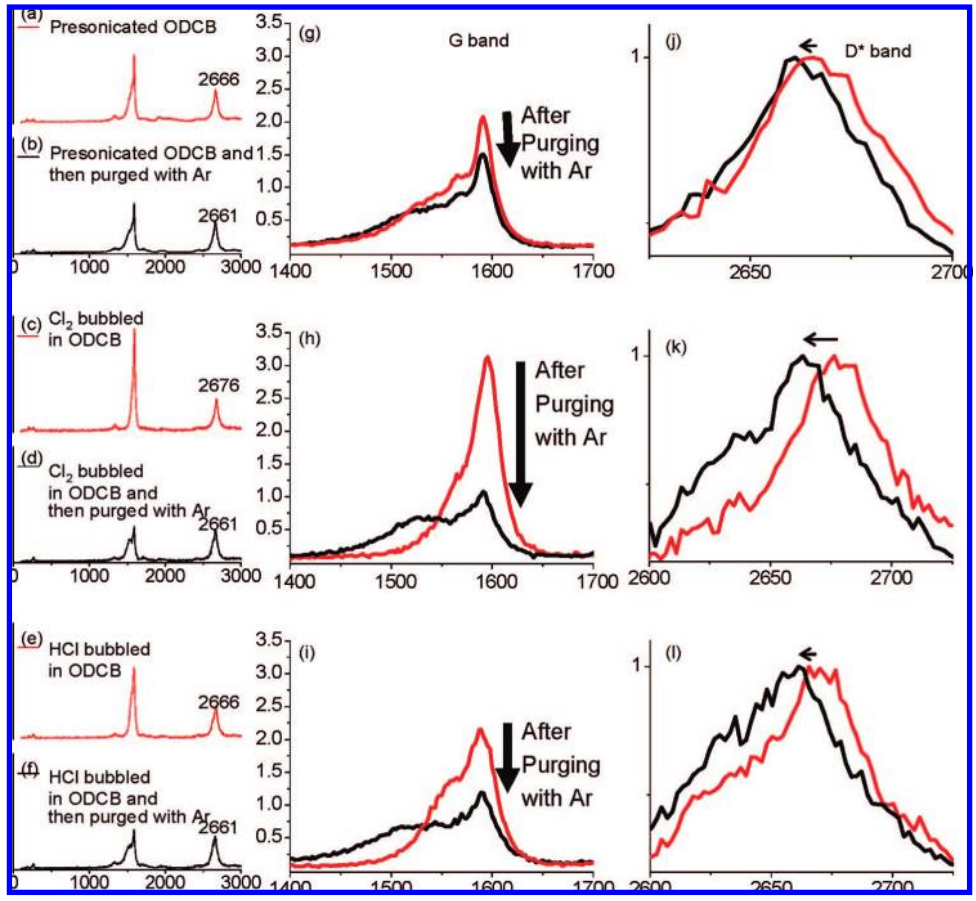

Figure 4. (Left) Raman spectra of SWCNTs stirred in (a) presonicated ODCB, (b) presonicated ODCB purged with Ar, (c) Cl_2 bubbled in ODCB, (d) same solvent mixture as used in (b) but purged with Ar, (e) HCl bubbled in ODCB, and (f) same solvent mixture as used in (e) but purged with Ar. (Right) Close-up views of the G band (g−i) and the D* band (j−l) of the samples in (a)−(f), respectively.

Table 1. Summary of the Effects of Solvents on the Raman Features of SWCNTs[a]

solvent + SWCNTs	G/D* ratio	lost shoulder	D* position (±2 cm^{-1})
annealed SWCNTs	1.3	no	2657
DCM	2.1	yes	2661
$CHCl_3$	1.7	yes	2663
1,2-DCE	1.7	yes	2663
CCl_4	1.4	no	2657
Cl-Ph	1.3	no	2657
1-Cl-But	1.2	no	2659
THF	1.0	no	2659
MeOH	1.4	no	2661
EtOH	1.4	no	2661
DMF	1.2	no	2657

[a] Full spectra are available in the Supporting Information, S4.

The interactions of SWCNTs in different solvents yield different dispersion states[62] after sonication. This results in different aggregation states or morphologies[57] after filtration, giving rise to the shift in Raman features.[56] However, the Raman spectra only consistently exhibit doping features for SWCNTs sonicated with DCM, $CHCl_3$, and 1,2-DCE (Table 1 and Supporting Information, S4). There is a shift in the D* peak coupled with a higher relative intensity in the G band along with a loss of asymmetry in the shoulder of the G band. Molecules such as DMF, EtOH, MeOH, THF, CCl_4, Cl-Ph, and 1-Cl-But do not show any change corresponding to doping such as a loss in asymmetry (loss of continuum states) of the shoulder or an increase in G band intensity. From our current experiments, only molecules with two or more chlorine atoms, such as DCM, $CHCl_3$, and 1,2-DCE, instigate doping. Along with the two chlorine atoms, they also have one or more hydrogen atom(s) present in the molecule. Only such molecules appear to produce enough Cl_2 and/or HCl(g) to initiate doping. For reasons that are unclear at this point, monochlorinated solvents such as Cl-Ph and 1-Cl-But, along with a fully chlorinated solvent (CCl_4), do not lead to any doping. This effect appears to be due to insufficient chlorine atoms on the former molecules and the absence of hydrogen in the latter.

3.6. Role of Iron Chlorides. The doping effect of ODCB on SWCNTs was examined by XPS. Changes in the Fermi-level position (E_F) caused by doping can be investigated by this method. In XPS, the binding energy (BE) is referenced to the Fermi-level position—a shift in the E_F is related to a change in the BE of the spectral features. The chemical binding environment of an element can be determined on the basis of the BE of the spectral features observed. Sonication of SWCNTs in ODCB changes the core-level spectra.

The ODCB treatment induces significant changes in the sample composition, such as the appearance of chlorine peaks (Supporting Information, S5). Two iron peaks are present in the high-resolution scan of the annealed SWCNTs, as can be seen in Figure 5a. They are assigned to elemental Fe (706.99 eV) and Fe_2O_3 (710.12 eV). The Fe and the Fe_2O_3 peaks agree

(62) Ham, H. T.; Choi, Y. S.; Chung, I. J. *J. Colloid Interface Sci.* **2005**, *296*, 216–223.

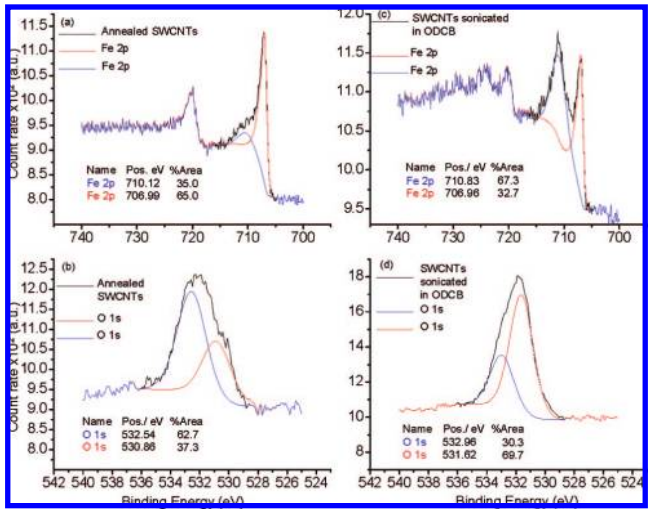

Figure 5. High-resolution spectra of (a) Fe 2p peaks for the annealed SWCNTs, (b) the O 1s peaks for the annealed SWCNTs, (c) the Fe 2p peaks for SWCNTs sonicated in ODCB, and (d) the O 1s peaks for SWCNTs sonicated in ODCB.

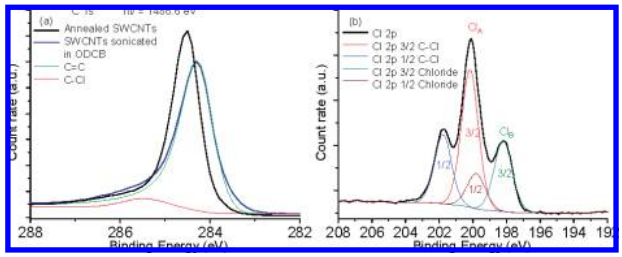

Figure 6. XPS high-resolution spectra of the (a) C 1s peak comparing annealed SWCNTs and SWCNTs sonicated in ODCB and (b) Cl 2p peaks of the sonicated sample.

with reported literature values.[63,64] From Figure 5b, the peak of the O 1s level is attributed to two species: the lower binding energy is assigned to O^{2-} (530.86 eV) while the other is ascribed to OH^- (532.54 eV). This agrees with the literature values for oxygen species.[64] After sonication, the spectral weight of the hydroxyl species increases, whereas that of the O^{2-} remains constant.

Figure 6a shows a high-resolution XPS spectrum of the C 1s peak, comparing the annealed SWCNTs to the SWCNTs sonicated in ODCB. A shift of 0.2 eV toward a lower BE is observed for the SWCNTs sonicated in ODCB, along with a broader line shape. The shift of the C 1s peak toward lower BE is related to the shift in the Fermi level. This is described as p-type doping; thus, the Fermi level is brought closer to the valence band edge. Wertheim and Citrin suggested that the asymmetry of the C 1s line shape is a function of the density of states (DOS) at the Fermi level.[65] When the DOS near the Fermi level changes, the C 1s line shape also changes. The presence of polymeric material accounts for the tailing observed in the C 1s (blue line) of SWCNTs sonicated in ODCB, as seen in Figure 6a. The polymeric material is capped with chlorinated benzene moieties, which explains the presence of C−Cl bonds.

The Cl 2p level of the sonicated SWCNTs is shown in Figure 6b. The Cl 2p core level binding energy appears as two inequivalent chemical environments. They exist as doublets associated with 3/2 and 1/2 levels, which are separated by 1.6 eV due to spin−orbit coupling.[66] The more intense peak, Cl_A, is associated with an organic C−Cl bond and appears at a core binding energy of 200.2 eV. The less intense component, Cl_B, present at a lower binding energy of 198.2 eV, is attributed to chloride ions.[66,67]

From our high-resolution XPS data of the SWCNTs sonicated in ODCB, the Fe ($2p_{3/2}$) is observed at 710.83 eV (Figure 5c), and the Cl^- peak is observed at 198.2 eV (Figure 6b). Thus, we have identified the species as being iron(II) chloride, formed during sonication. The Fe^{2+} ($2p_{3/2}$) and Cl^- ($2p_{3/2}$) peaks are commonly observed at 710.8 eV[68] and 198.4 eV,[69] whereas the Fe^{3+} ($2p_{3/2}$) and Cl^- ($2p_{3/2}$) peaks are commonly observed at 711.5 eV[68] and 199.0 eV,[69] respectively. The dopant $FeCl_3$, being an electron acceptor, appears as Fe^{2+} because of charge transfer due to p-doping. Therefore, iron(III) chloride could also be present. Hydrogen chloride and chlorine present in the sonicated sample react with the catalytic Fe nanoparticles initially present. Iron chlorides are hygroscopic and form hydrated compounds due to exposure to air during transfer to the XPS chamber. This also explains the increase in spectral weight of the hydroxyl species (Figure 5d).

We cannot neglect the formation of iron(III) chloride. Its hydrated complex has a low melting point of 37 °C, at which it is reported to decompose[70] via heating or reduction. Decomposition produces chlorine, hydrogen chloride, chlorides, and iron oxides when the complex is heated in air. Elemental Fe is present in the SWCNTs; since $FeCl_3$ reacts readily with metals, Fe reduces $FeCl_3$ to $FeCl_2$. It has been reported that iron(II) chloride is produced by refluxing iron(III) chloride in ODCB[71] according to the following equation:

$$C_6H_4Cl_2 + 2FeCl_3 \rightarrow C_6H_3Cl_3 + 2FeCl_2 + HCl$$

During sonication, a temperature of 32−38 °C is reached, thus enabling the formation of $FeCl_2$ (deduced from XPS results) and trichlorobenzenes (detected from GC-MS, Supporting Information, S2). Previously, only $FeCl_3$ has been shown to dope SWCNTs.[30] We show, in Figure 7b,c, that both $FeCl_2 \cdot 4H_2O$ and $FeCl_3 \cdot 6H_2O$ dope the SWCNTs when they are stirred in methanol. Methanol is used as solvent because it does not lead to doping and readily dissolves the iron chlorides. The results indicate a loss in continuum of the G band and an upward shift in the D* peak by 13 cm^{-1}, in comparison to the equivalent peak (2657 cm^{-1}) for the annealed SWCNTs (Figure 7a).

A new batch of HiPco SWCNTs (NB-SWCNTs) with a lower total residual mass of 5 wt % was used to investigate the effect of a lower catalytic iron content. The Fe content was found by heating the SWCNTs (1 mg) using a TGA (Supporting Information, S6) to 1100 °C, and the residue was digested with 26 wt % chloric acid. The residual catalytic content of the NB-SWCNTs was determined by ICP-MS to be 1.9 μg/mL in 25 mL of 1 wt % HNO_3, which is equivalent to 5 wt % Fe. The Fe

(63) Wandelt, K. *Surf. Sci. Rep.* **1982**, *2*, 1–121.
(64) Mills, P.; Sullivan, J. L. *J. Phys. D: Appl. Phys.* **1983**, *16*, 723–732.
(65) Wertheim, G. K.; Citrin, P. H. In *Photoemission in Solids I: General Principles*; Cardona, M., Ley, L., Eds.; Springer-Verlag: Berlin, 1978; pp 197−234.
(66) Beamson, G.; Briggs, D. *High-Resolution XPS of Organic Polymers*; John Wiley & Sons Ltd.: Chichester, 1992.
(67) Papirer, E.; Lacroix, R.; Donnet, J.-B.; Nanse, G.; Fioux, P. *Carbon* **1995**, *33*, 63–72.
(68) Carver, J. C.; Schweitzer, G. K.; Carlson, T. A. *J. Chem. Phys.* **1972**, *57*, 973–982.
(69) Kishi, K.; Ikeda, S. *J. Phys. Chem.* **1974**, *78*, 107–112.
(70) Lide, D. R. Physical constants of inorganic compounds. In *CRC Handbook of Chemistry and Physics*, 87th ed.; Lide, D. R., Eds.; Taylor and Francis: Boca Raton, FL, 2007; Internet Version, 4-43−4-101.
(71) Kovacic, P.; Brace, N. O. *J. Am. Chem. Soc.* **1954**, *76*, 5491–5494.

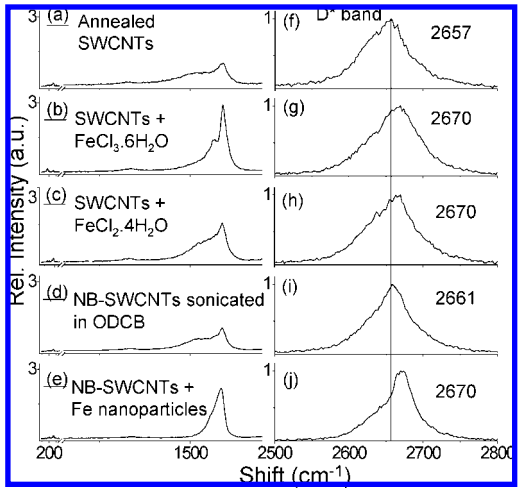

Figure 7. (Left) Raman spectra of (a) annealed SWCNTs, and (b,c) SWCNTs respectively stirred with 10 wt % $FeCl_3 \cdot 6H_2O$ and 10 wt % $FeCl_2 \cdot 4H_2O$ in methanol, (d) NB-SWCNTs sonicated in ODCB, and (e) NB-SWCNTs spiked with 10 wt % Fe nanoparticles and then sonicated in ODCB. (Right) Close-up views of the D* bands, (f)−(j), for samples (a)−(e), respectively.

content is lower than in the batch of HiPco previously used. The previous batch was determined to have 5.6 μg/mL of Fe in 25 mL of 1 wt % HNO_3, which is equivalent to 14 wt % Fe. The NB-SWCNTs did not exhibit any doping behavior when sonicated with ODCB, as shown in Figure 7d. This further ascertains that doping is dependent on the Fe content accessible for reaction during sonication. With a 5 wt % residual mass, not only is the Fe content lower, but this also implies that the purification technique cannot completely remove the Fe. Therefore, the remaining catalytic material is also less susceptible to further reaction. Accretion of Fe along the tube is known to occur during synthesis,[5] contributing to the level of impurity; therefore, these Fe nanoparticles are more accessible for reaction during sonication. To confirm this, we added Fe_2O_3 nanopowder (0.1 mg) to the NB-SWCNTs (1.0 mg), spiking the Fe content to 10 wt % above its initial value. This mixture was then sonicated in ODCB, and the result is shown in Figure 7e. Addition of Fe nanoparticles to the NB-SWCNTs and sonication in ODCB led to doping. The G band lost its shoulder, and the D* peak (Figure 7j) is up-shifted by 9 cm^{-1} with respect to Figure 7i. We conclude that the formation of iron chlorides is the cause of doping in the SWCNTs, thereby altering the spectrum.

4. Conclusion

The electronic band structure of SWCNTs is disrupted by sonication in chlorinated solvents in the presence of Fe nanoparticles. Sonicating HiPco SWCNTs (14 wt % total residual mass) in solvents such as ODCB, DCM, $CHCl_3$, and 1,2-DCE leads to p-type doping. Sonication not only is routinely used to disperse SWCNTs but also inevitably decomposes the solvent to form new species such as hydrogen chloride and chlorine gases. These, in turn, react with the Fe nanoparticles to form iron chlorides. This doping behavior was characterized by a loss in the shoulder of the G band, an increase in relative intensity of the G band, and an upward shift of the D* mode in the Raman spectra of SWCNTs. XPS data of the C 1s showed a shift to lower BE that also validates charge-transfer leading to this p-type doping behavior. Therefore, we conclude that residual catalytic impurities influence the underlying chemistry of SWCNTs during a wet-chemical process. Our research brings into perspective the interaction of the catalytic impurities with the solvent, which can explain a shift in the Raman spectrum as previously noted by Cooper et al.[72] Our study provides a platform on which future work, such as intentional doping of the SWCNTs using ionic liquids or salts for use in molecular electronics, can be achieved. We are currently working on using p-type doping to exfoliate and disperse SWCNTs in order to enhance their bulk processability and to investigate the reactivity of the side walls during sonication.

Acknowledgment. We are grateful to Adam P. Hitchcock, Alex Adronov, and Maria Abou Chakra for fruitful discussion; Leah Allan for help with GC-MS; Kirk Green and Stephen Yue Wang for help with MALDI-TOF; Patricia Martin, Karen Neumann, Heather Petit, Nicki Robinson, Angela Vanderlaan, and Janet Welsh for help with logistics (all McMaster University); Kevin Fergusson (Occupational and Environmental Health Laboratory) for help with ICP-MS; Jim Garrett for help with annealing SWCNTs; Frank Gibbs (Brockhouse Institute for Materials Research) for help with TGA; Gregoryz Szymanski (Electrochemical Technology Laboratory, Guelph) for help with Raman spectroscopy; and Mark Biesinger (Surface Science Western) for help with XPS. The work was financially supported by the Natural Science and Engineering Research Council of Canada and an Ontario Premier's Research Excellence Award.

Supporting Information Available: Additional Raman spectra, GC-MS, XPS, and TGA data, along with a list of chemicals used (with a certificate of analysis for ODCB). This material is available free of charge via the Internet at http://pubs.acs.org.

JA8036788

(72) Cooper, C. A.; Young, R. J. Investigation of the Deformation of Carbon Nanotube composites Through the Use of Raman Spectroscopy. In *Science and Application of Nanotubes*; Tománek, D., Enbody, R. J., Eds.; Kluwer Academic/Plenum Publishers: New York, 2000.